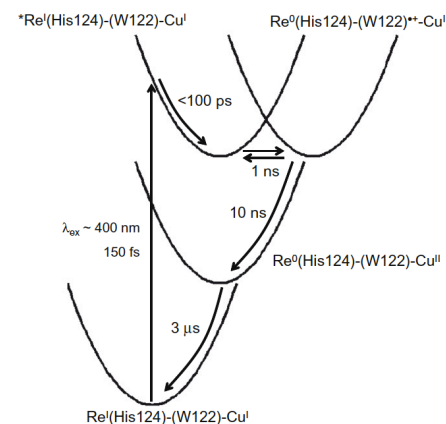
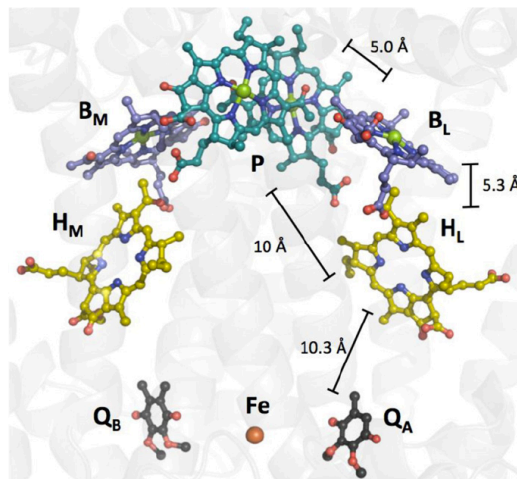
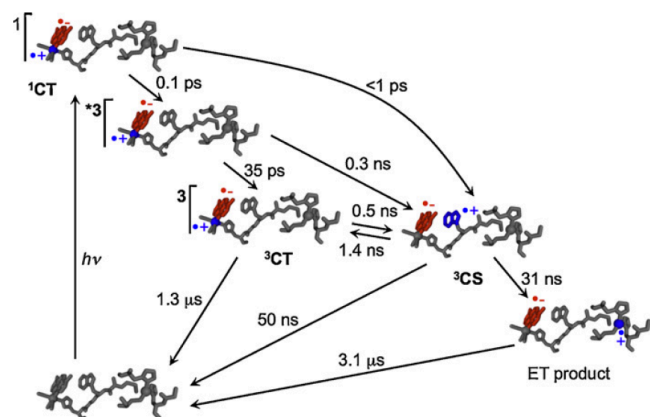




The Career of Harry B. Gray:

Efficient Electron Transfer in Natural Redox Machines

MacMillan Group Meeting
February 13, 2013
Robert J Comito



CV of Harry B. Gray



♦Education

- 1957 B.S. Western Kentucky State University
- 1960 PhD Northwestern University with Fred Basolo and R.G. Pearson
- 1960-1961 NSF Postdoctoral Fellow at the University of Copenhagen with C.J. Ballhausen

♦Notable awards

- 1986 National Medal of Science
- 1991 Priestly Medal (American Chemical Society)
- 2000 Harvey Prize (Technion-Israel Institute of Technology)
- 2004 Wolf Prize for Chemistry
- 2009 Welch Award for Chemistry

♦Famous Students: Dan Nocera (MIT), Herbert Holden Thorp (UNC Chapel Hill), Mark Stephen Wrighton (WSU St Louis)



CV of Harry B. Gray



Beckman Institute Laser Resource Center



♦Honorary appointments

- American Academy of Arts and Sciences (member 1979, fellow 1989)
- Royal Academy Göteborg (foreign member 1995)
- Royal Society of Great Britain (foreign member 2000)
- Royal Society of Chemistry (honorary fellow 2005)
- ACS fellow (2009)

♦Academic positions

- Columbia University (1960-1966)
- California Institute of Technology (1966-present)
- Arnold O. Beckman Professor of Chemistry (1981-present, Caltech)
- Founding director of Beckman Institute and Principal Investigator at the B.I. Laser Resource Center
- Solar fuels director at CCI Solar (aka, General of the Solar Army)

A Prolific Postdoc

The Electronic Structure of the Vanadyl Ion¹

By C. J. BALLHAUSEN AND HARRY B. GRAY²

Received October 2, 1961

The bonding in the molecule ion $\text{VO}(\text{H}_2\text{O})_6^{2+}$ is described in terms of molecular orbitals. In particular, the most significant feature of the electronic structure of VO^{2+} seems to be the existence of considerable oxygen to vanadium π -bonding. A molecular orbital energy level scheme is estimated which is able to account for both the "crystal field" and the "charge transfer" spectra of $\text{VO}(\text{H}_2\text{O})_6^{2+}$ and related vanadyl complexes. The paramagnetic resonance g factors and the magnetic susceptibilities of vanadyl complexes are discussed.

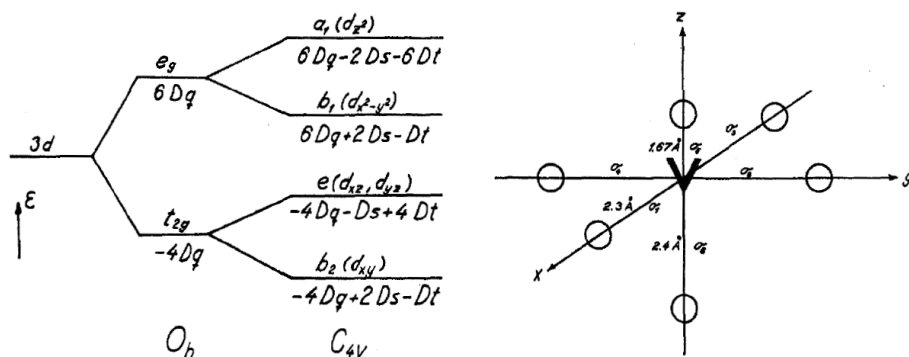
Inorg. Chem. **1962**, *1*, 111-122.

"The Ballhausen-Gray model for metal-oxo bonding remains the standard to this day...enabl[ing] a generation of computational chemists to perform molecular orbital calculations of the structures and reactivities of inorganic molecules."

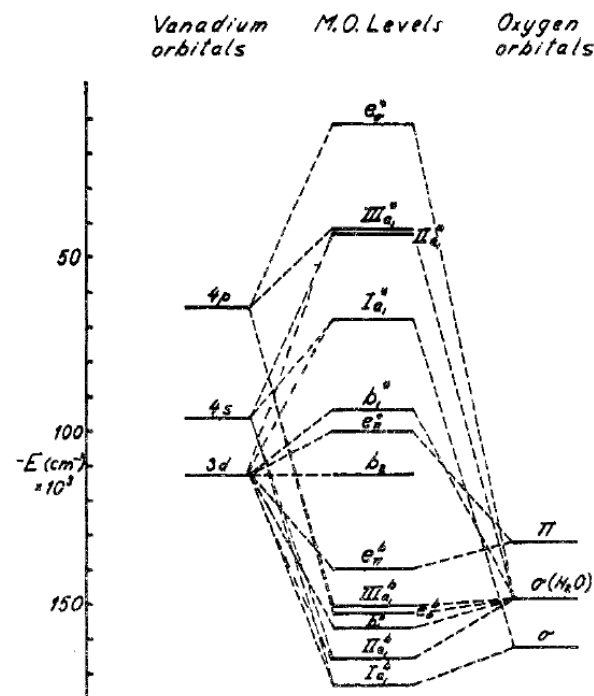
Jay R Winkler (former Gray student and collaborator at BILRC)
"A Celebration of Harry B Gray's 75th Birthday" *Coor. Chem.*
Rev. **2011**, *255*, 617-618.

Electronic Structure of the Vanadyl Ion

- ♦ A ligand field model of vanadyl ion (VO^+) is inconsistent with magnetic and spectroscopic measurements
- ♦ A symmetry based MO treatment of VO^+ accurately predicts the observed electronic energy levels



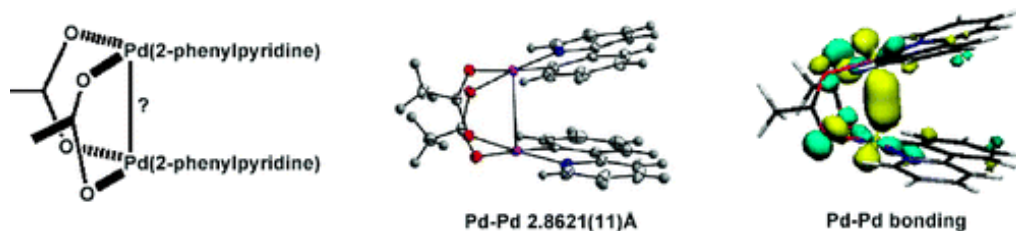
A ligand field description of $\text{VO}(\text{OH}_2)_5^+$



Ballhausen-Gray MO description of $\text{VO}(\text{OH}_2)_5^+$

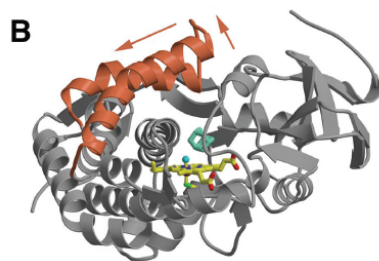
Longstanding Research Interests

Bonding in metal complexes:



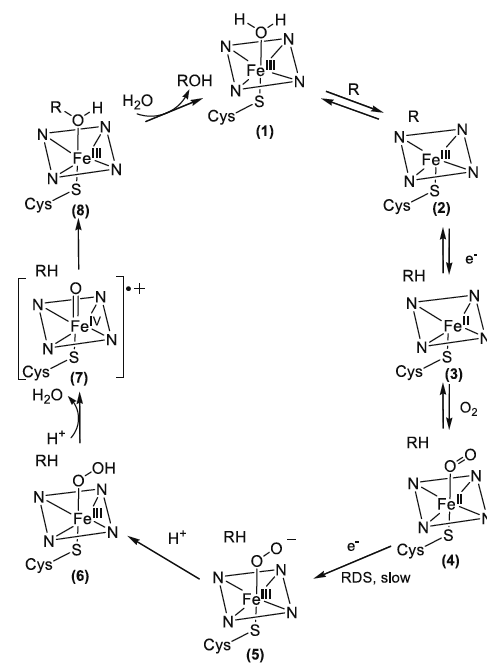
Bercaw, J.E.; Durrell, A.C.; Gray, H.B.; Green, J.C.; Hazari, N.
Inorg. Chem. **2010**, *49*, 1801-1810.

Dynamics of protein folding and unfolding:



Dunn, A.R.; Dmochowski, I.J. Bilwes, A.M.; Gray, H.B.; Crane, B.R.;
Proc. Natl. Acad. Sci. **2001**, *98*, 12420-12425.

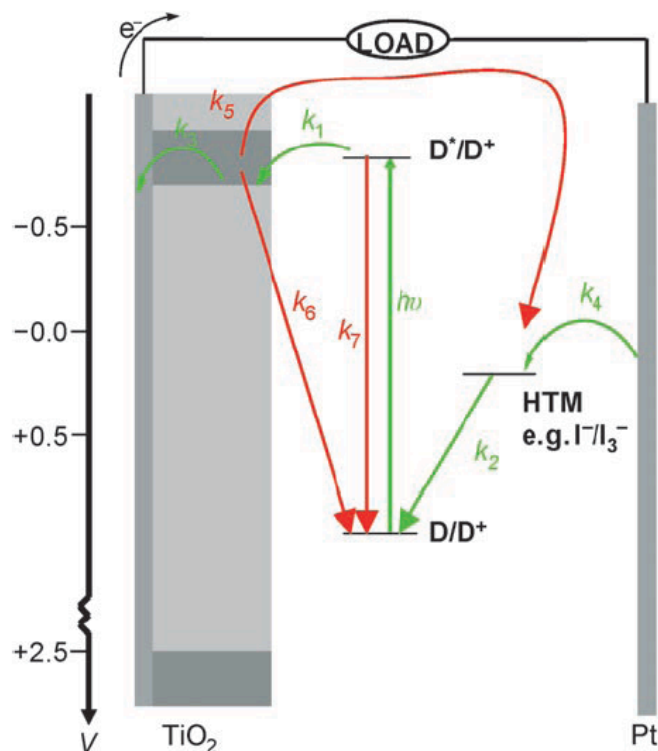
Bioinorganic reaction mechanisms:



Contakes, S.M. Le Nguyen, Y.H.; Gray, H. B.; Glazer, E.C.; Hays, A. M.; Goodin, D.
B. Struct. Bond. **2007**, *123*, 177-203

Dye-Sensitized Solar Cells (DSSCs)

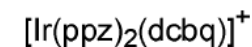
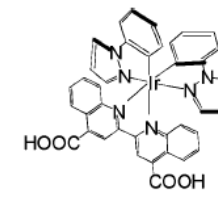
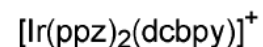
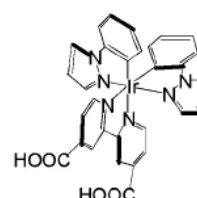
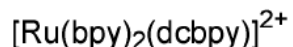
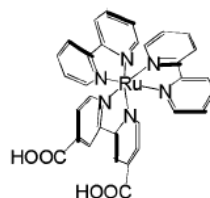
Outline of DSSC operation:



TiO₂: a cheap, abundant band gap material

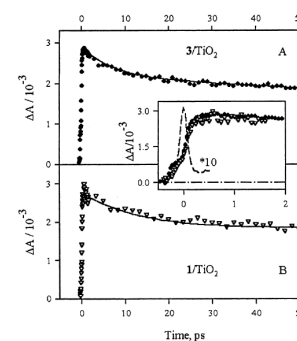
Robertson, N. *Angew. Chem. Int. Ed.* **2006**, 45, 2338-2345.

Using LLCT excitation improves charge separation and reduces nonproductive charge recombination:



Photochem. & Photobiol. **2006**, 5, 871-873.

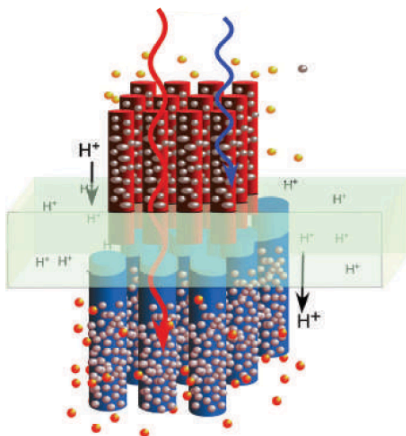
Efficient electron injection depends on picosecond electron transfer from dye to TiO₂ valence band



J. Phys. Chem. B. **2002**, 106, 9347-9358.

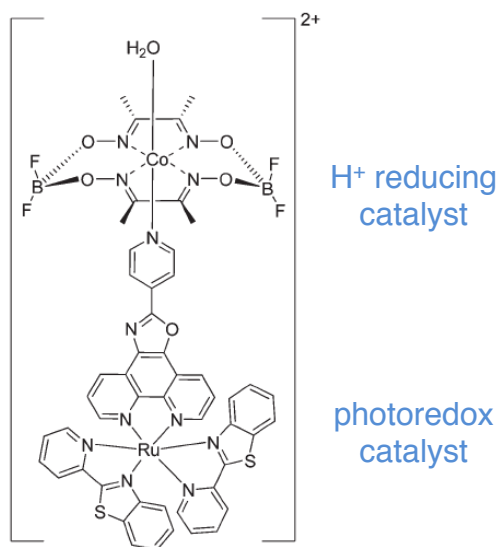
Catalysts for Efficient Water Splitting

Solar materials for hydrogen production:



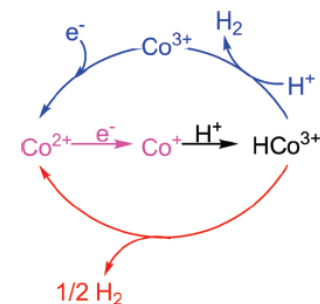
Gray, H.B. *Nat. Chem.* **2009**, *1*, 7.

Molecular catalysts for photolytic hydrogen:



Dalton Trans. **2012**, *41*, 13060-13073.

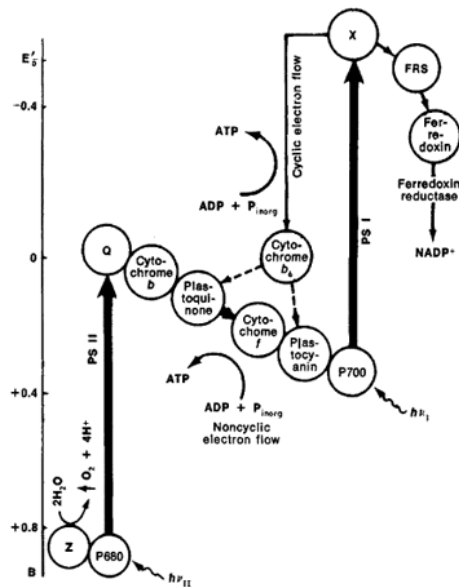
Mechanism of water splitting:



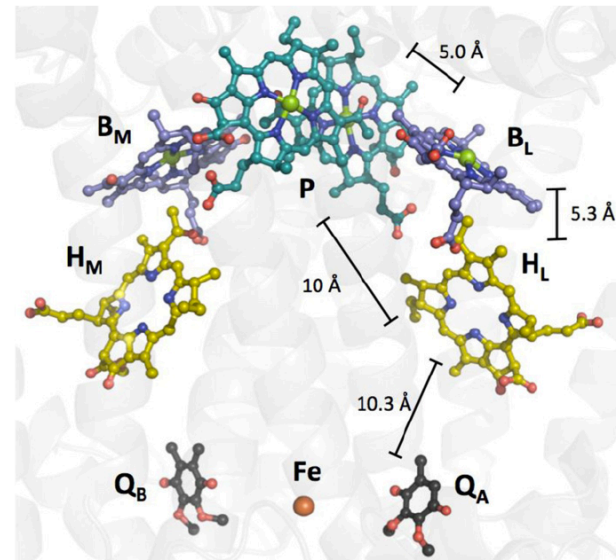
J. Am. Chem. Soc. **2010**, *132*, 1060-1065

A major theme: design features for efficient electron transfer

This Talk: Electron Transfer in Natural Systems



Energy diagram for photosynthesis

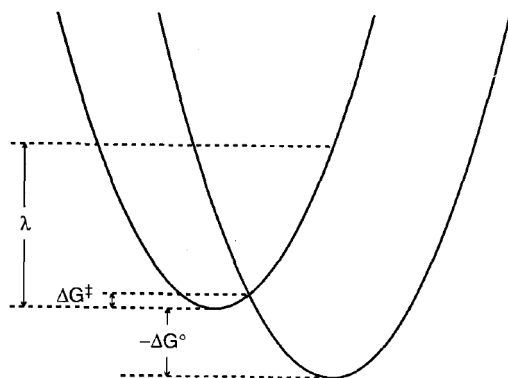


Bacterial photosynthetic redox center: an efficient natural redox machine

- ◆ In order for complex biochemical processes to be efficient, electron transfer (ET) must:
 - Be fast and cover great distances
 - Have high directional control
 - Have small – ΔG associated with individual steps

What controls the efficiency of ET in natural redox machines?

Electron Transfer Theory



$$k_{ET} = \left(\frac{4\pi^3}{h^2 \lambda k_B T} \right)^{1/2} H_{AB}^2 e^{- (\Delta G^\circ + \lambda)^2 / 4 \lambda k_B T}$$

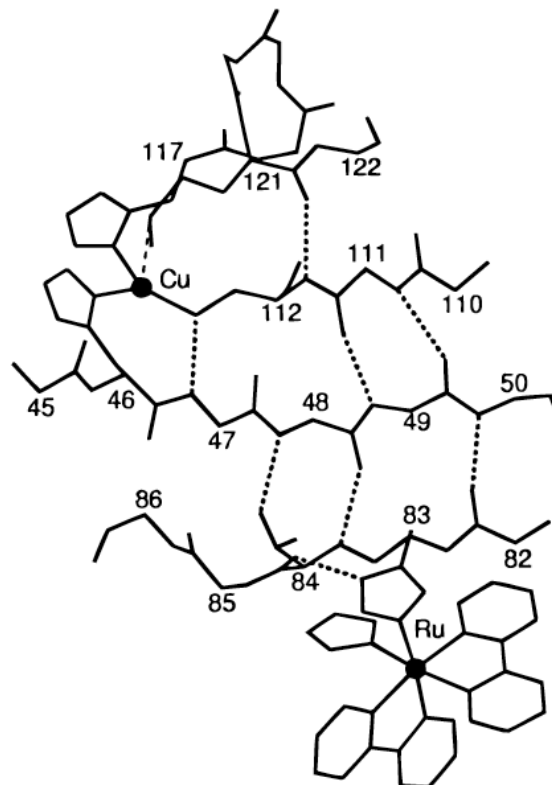
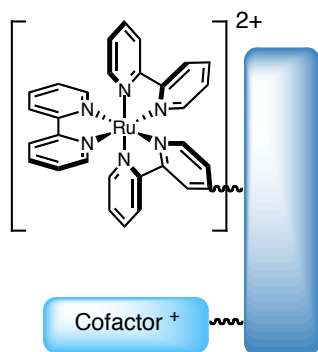
For a semiclassical description of tunneling

- ♦ Reorganization energy (λ)
 - The energy of the reactants at equilibrium nuclear configuration of products
 - Changes in solvation, coordination, and conformation upon electron transfer all will increase λ
 - Electron transfer fastest when $-\Delta G = \lambda$
- ♦ Weak dependence of k_{ET} on absolute temperature (T)
 - Small drops in rate at cryogenic T usually indicates tunneling mechanism
- ♦ Electronic coupling (H_{AB} , QM definition)
 - Measure of orbital overlap, distance, and ability of intervening medium to transmit electrons

Laser Flash Quench Studies

Design plan:

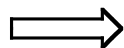
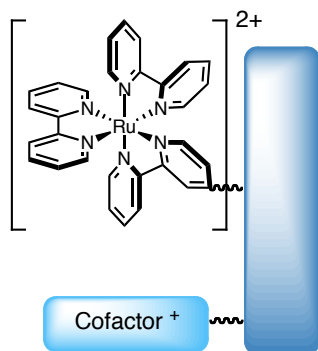
bioconjugation of
photocatalyst



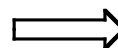
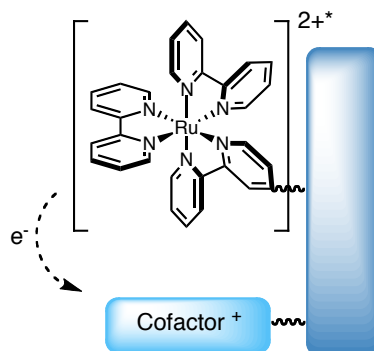
Laser Flash Quench Studies

Design plan:

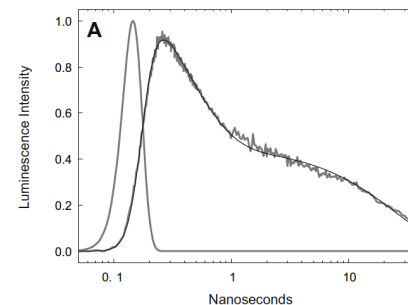
bioconjugation of
photocatalyst



laser pulse
photoexcitation

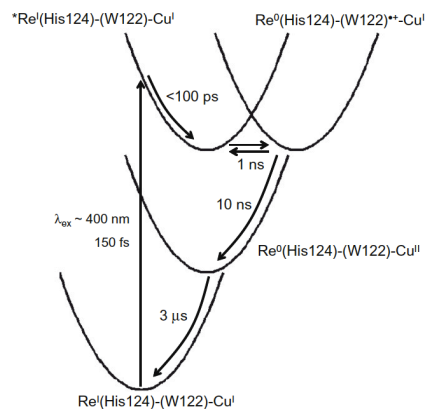
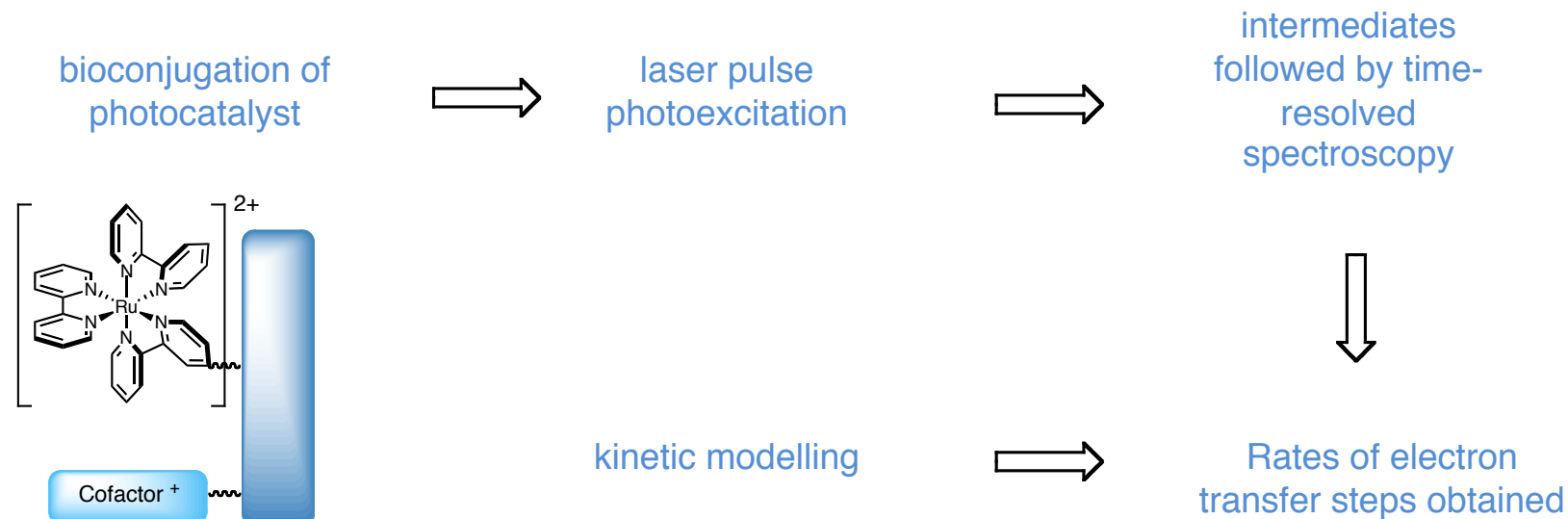


intermediates
followed by time-
resolved
spectroscopy



Laser Flash Quench Studies

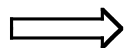
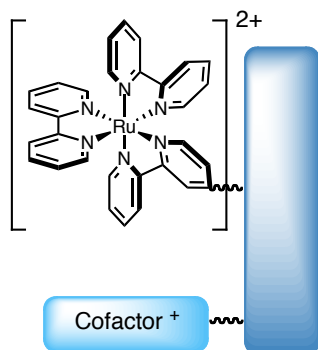
Design plan:



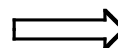
Laser Flash Quench Studies

Design plan:

bioconjugation of photocatalyst



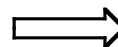
laser pulse photoexcitation



intermediates followed by time-resolved spectroscopy



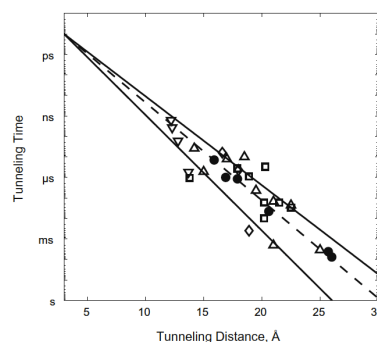
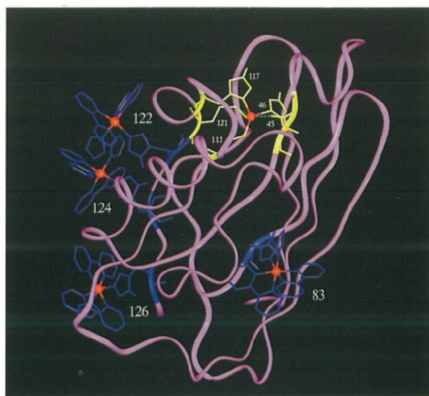
kinetic modelling



Rates of electron transfer steps obtained

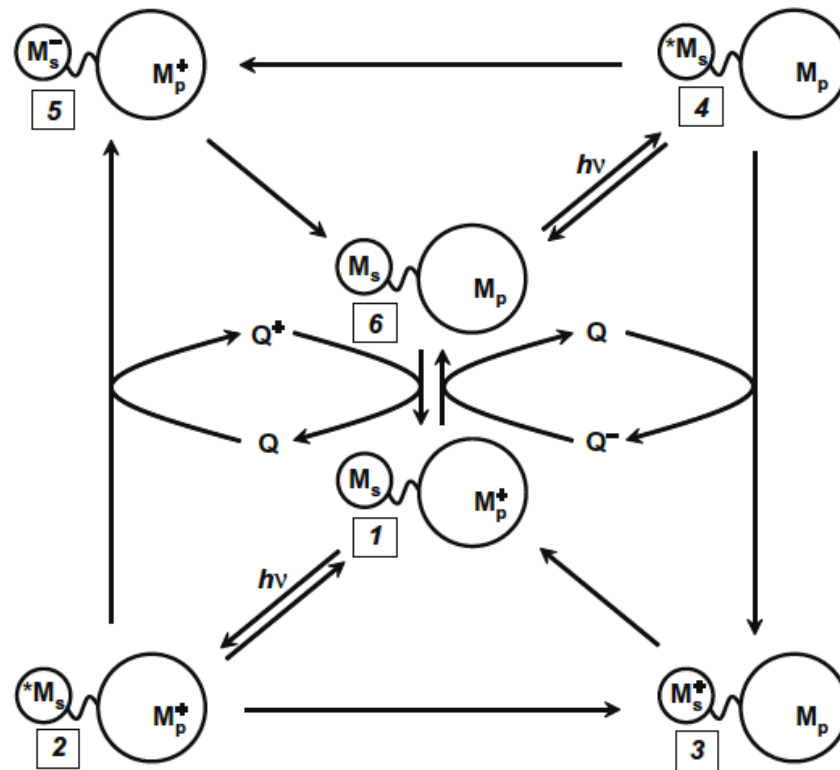


Structural variation provides trends in ET rates

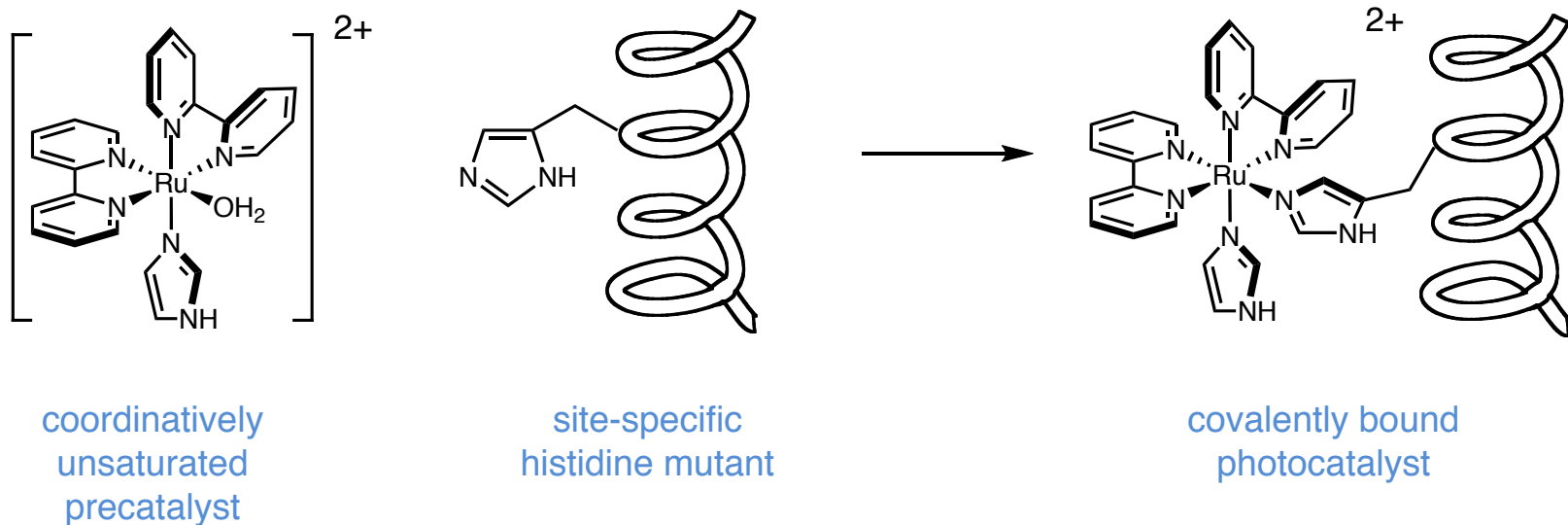


Laser Flash Quench Studies

Design plan:



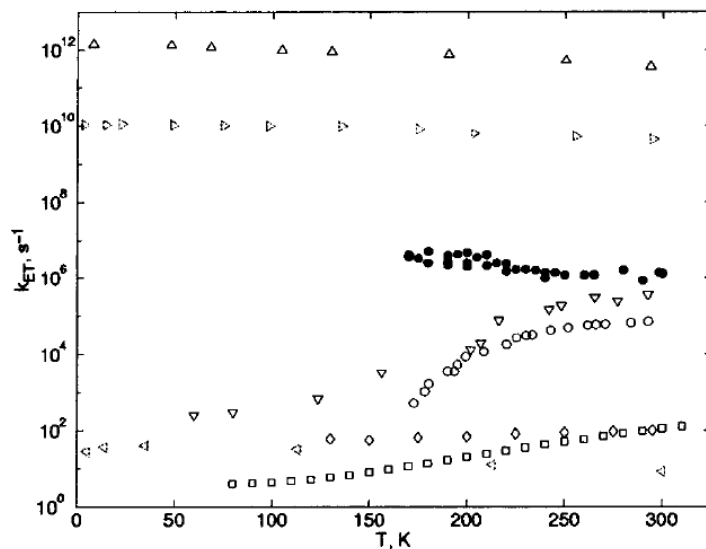
Bioconjugation of Photocatalysts



- ♦ Choice of photocatalyst to optimize ΔG and λ
- ♦ Follow catalyst oxidation state and excitation state by time resolved spectroscopy
 - UV/Vis, luminescence for bpy, terpy, phenanthroline complexes
 - IR for carbonyl complexes, e.g. $\text{Re}(\text{phen})(\text{CO})_3(\text{His})^+$

Temperature Dependence of k_{ET}

- ♦ In photosynthetic reaction center (PRC), primary ET rate is same over large temperature range
 - Cooling from 300K to 4K, primary ET rate increases by a factor of 3



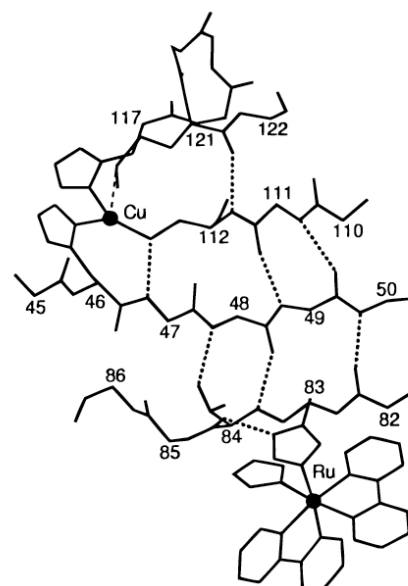
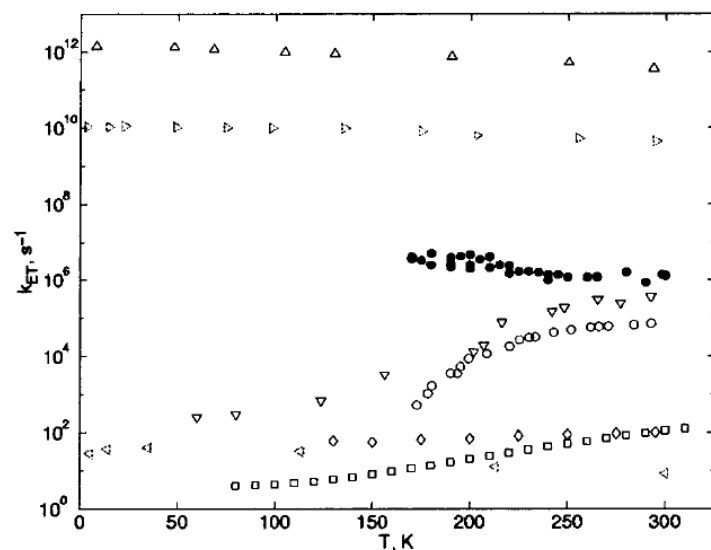
R. viridis primary charge separation in PRC

R. sphaeroides reduced quinone to oxidized special pair transfer in PRC

A more representative temperature trend among common ET enzymes

Temperature Dependence of k_{ET}

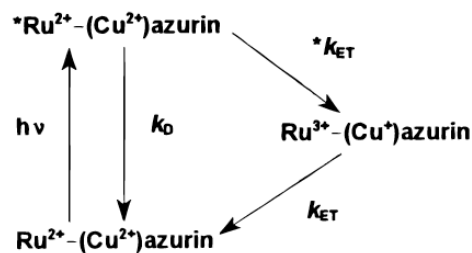
- ♦ In photosynthetic reaction center (PRC), primary ET rate is same over large temperature range
 - Cooling from 300K to 4K, primary ET rate increases by a factor of 3
- ♦ Model system: Ru-modified *P. aruginosa* azurins,
 - Azurins are blue copper proteins involved in bacterial arsenic metabolism
 - Ru(bpy)₂(im)(His83)azurin fixes photocatalyst and Cu reaction center across a beta sheet



Reaction center of
Ru(His83)azurin

Temperature Dependence of k_{ET}

- ♦ Laser flash quench studies follow modeled temperature trend down to 240K
- ♦ Significant increase in rate at cryogenic temperatures not explained by any model assuming constant λ , ΔG , and H_{AB}
 - Temperature dependence of one of these parameters



$$k_{ET} = \left(\frac{4\pi^3}{h^2 \lambda k_B T} \right)^{1/2} H_{AB}^2 e^{- (\Delta G^\circ + \lambda)^2 / 4 \lambda k_B T}$$

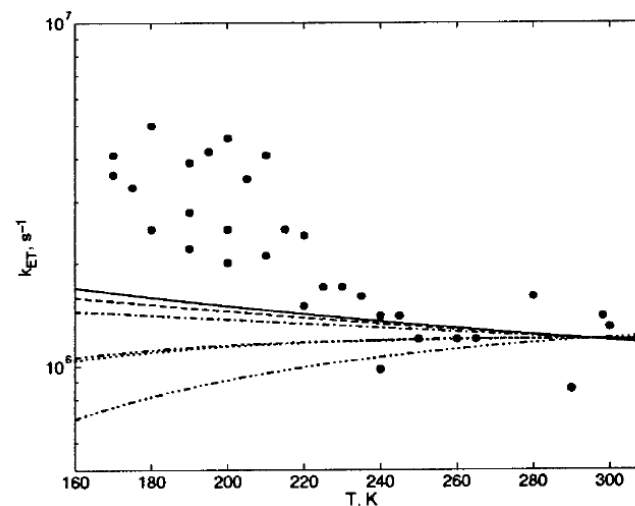
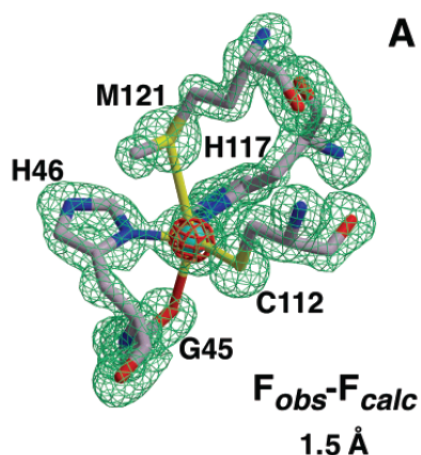


Figure 2. Variation of k_{ET} with temperature in Ru(His83)-azurin. The smooth lines were generated using eq 1 with $H_{AB} = 0.07 \text{ cm}^{-1}$ and λ values of 0.5 (···), 0.6 (---), 0.7 (—), 0.8 (—·—), 0.9 (— · — · —), and 1.0 eV (— · — · —).

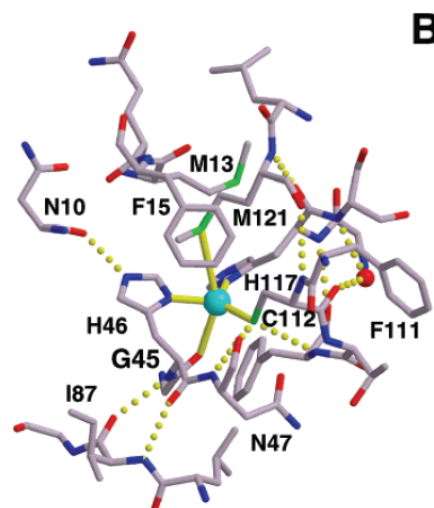
What accounts for the anomalous cryogenic increase in reaction rate?

Electron Tunneling in Single Crystals

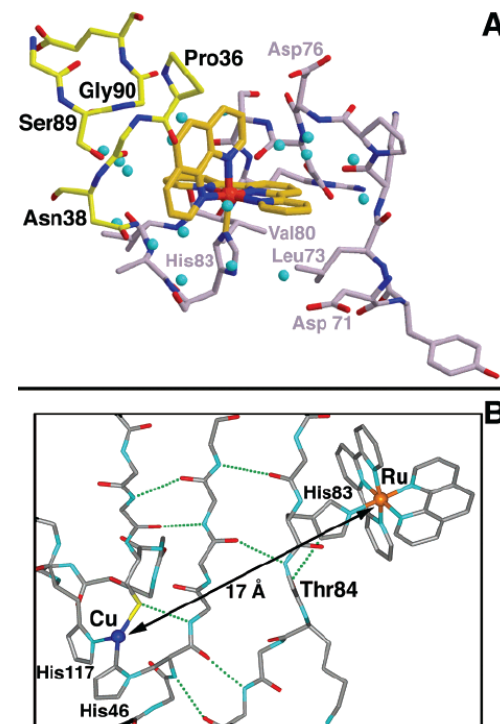
- ♦ For family of photocatalyst-bound azurins, rate in crystal is similar to that in solution
- ♦ Structural comparison in Cu(I) and Cu(II) proteins reveals minor change in bond distances
 - Redox active center well shielded from solvent



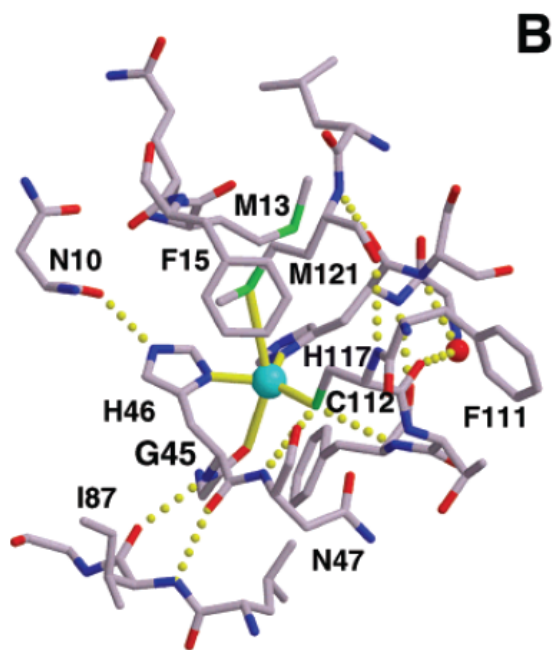
Coordination bond
distances change <
0.08 Å between Cu(I)
and Cu(II)



Low solvent accessibility at
active site



Electron Tunneling in Single Crystals



Hydrogen bonding network
distributes small structural
changes about protein

Conclusions:

- ♦ Fixed coordination and solvent exclusion minimize λ
 - Confirmed by large self-exchange reaction
 - Essential for fast ET with low $-\Delta G^\circ$
- ♦ More compact structure at low T further minimizes λ , accounting for cryogenic increase in k_{ET} .

But minimizing λ comes at a price:

- ♦ Burying redox cofactors in proteins means that electron transfer must occur at great distances between redox partners

Distant Electronic Coupling

$$k_{\text{ET}} = \left(\frac{4\pi^3}{h^2 \lambda k_{\text{B}} T} \right)^{1/2} H_{\text{AB}}^2 e^{- (\Delta G^\circ + \lambda)^2 / 4 \lambda k_{\text{B}} T}$$

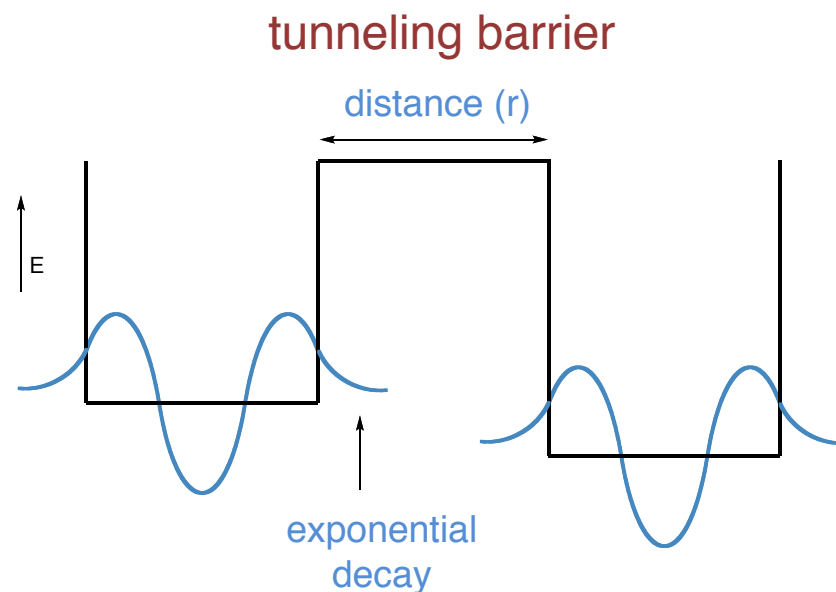
Rate strongly dependent on H_{AB}

♦ For square barrier tunneling model (constant barrier height) H_{AB} decays exponentially with distance:

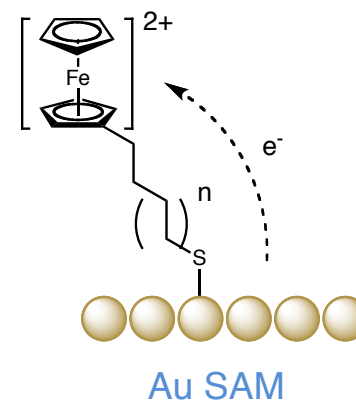
$$H_{\text{AB}}(r) = H_{\text{AB}}(r_0) e^{-\beta (r-r_0) / 2}$$

♦ Decay constant (β) depends on barrier height

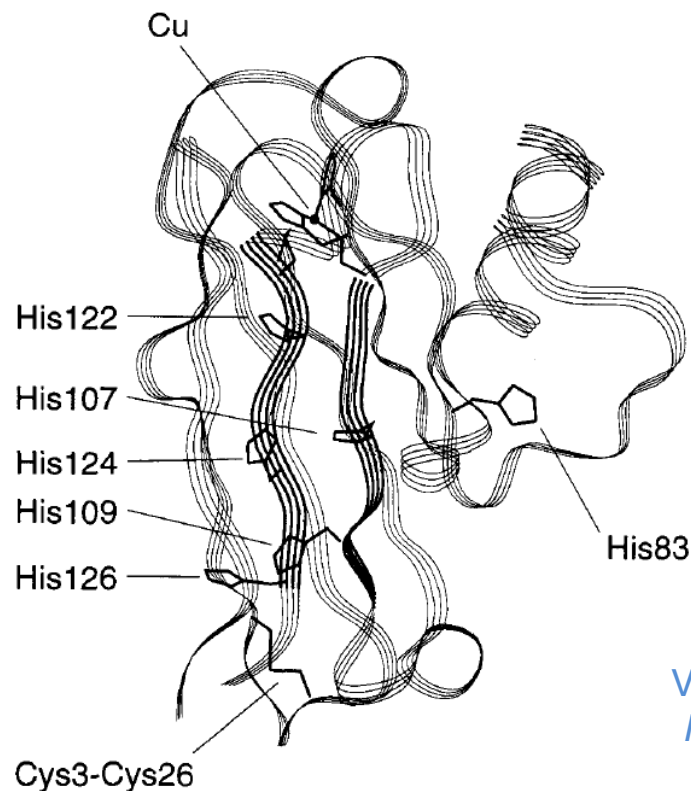
- $\beta = 3\text{--}5 \text{ \AA}^{-1}$ in a vacuum
- $\beta = 1.7 \text{ \AA}^{-1}$ in a H_2O
- $\beta = 1.0 \text{ \AA}^{-1}$ across a saturated alkane



Smalley
et al. :



Measuring Distance Dependence



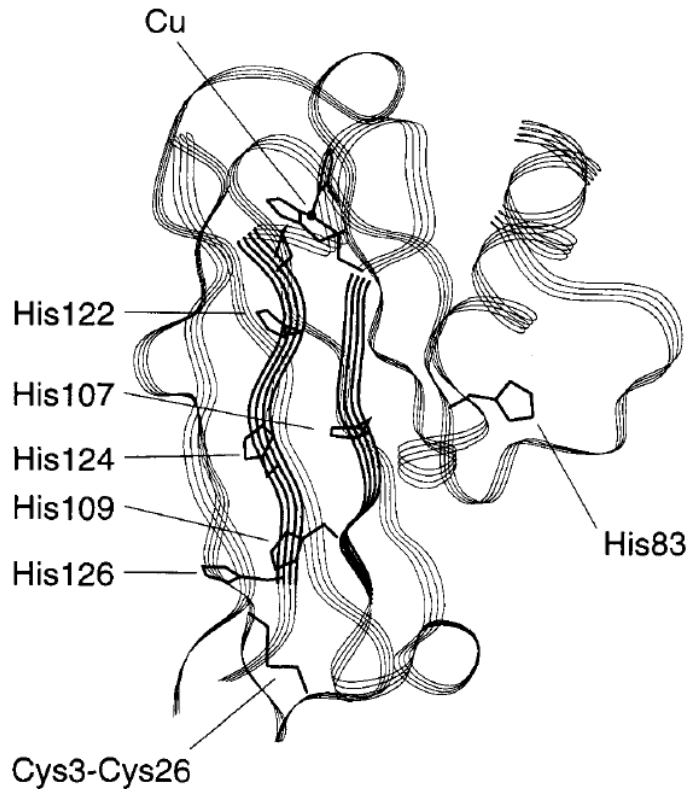
Design Plan:

- ♦ Prepare a family of photocatalyst-bound proteins with systematically donor-acceptor distances (constant λ , ΔG° , and $H_{AB}(r_0)$)
- ♦ Measure k_{ET} and determine decay constants (β)

Various histidine substituted mutants of
P. aeruginosa azurins for coordination
with $Ru(bpy)_2(im)^{2+}$

How does intervening protein structure affect electronic coupling (H_{AB})?

Measuring Distance Dependence



intercept =
rate at VDW
contact

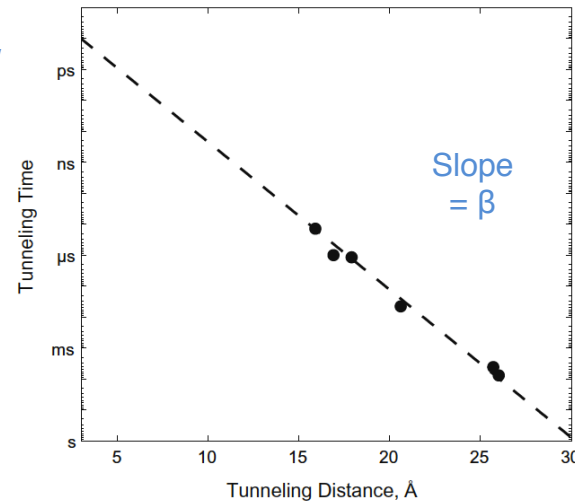
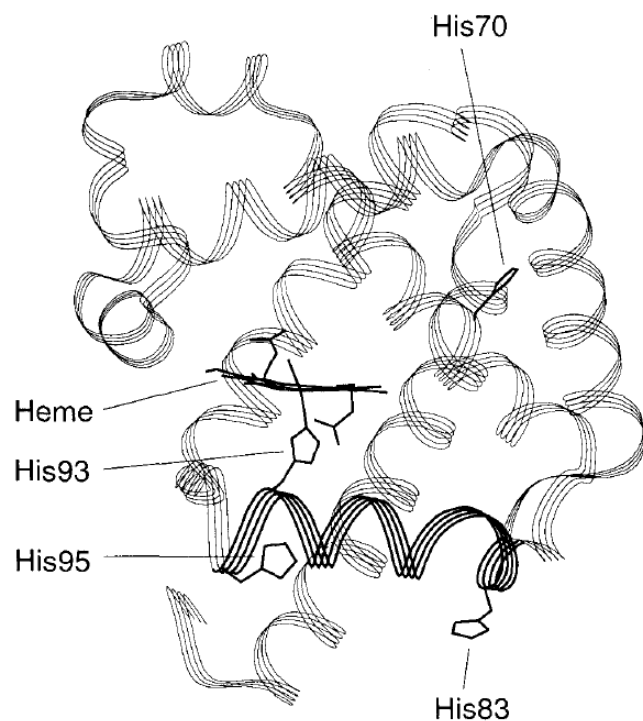


Fig. 2. Distance dependence of driving-force-optimized ET rates in Ru-labeled *P. aeruginosa* azurin. The dashed line is the best fit to the data ($\beta = 1.1 \text{ Å}^{-1}$).

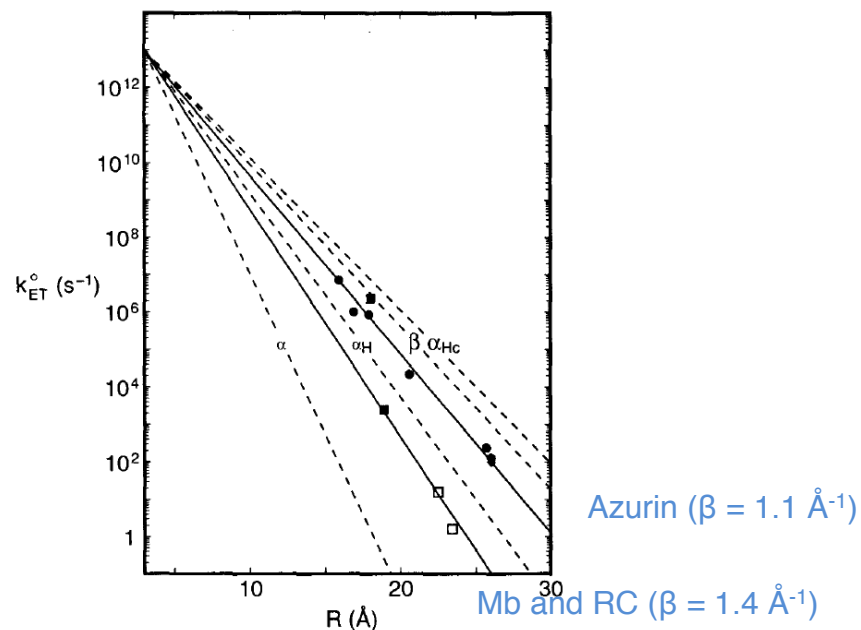
Result:

- ♦ Obtained $\beta = 1.1 \text{ Å}^{-1}$ for a azurin ET
- ♦ Hopfield et al. predicts $\beta = 1.4 \text{ Å}^{-1}$ for square tunneling barrier view of protein (ie, does not account for secondary structure)
- ♦ Azurin structure dominated by β -sheet

Distance Dependence on an α -Helix

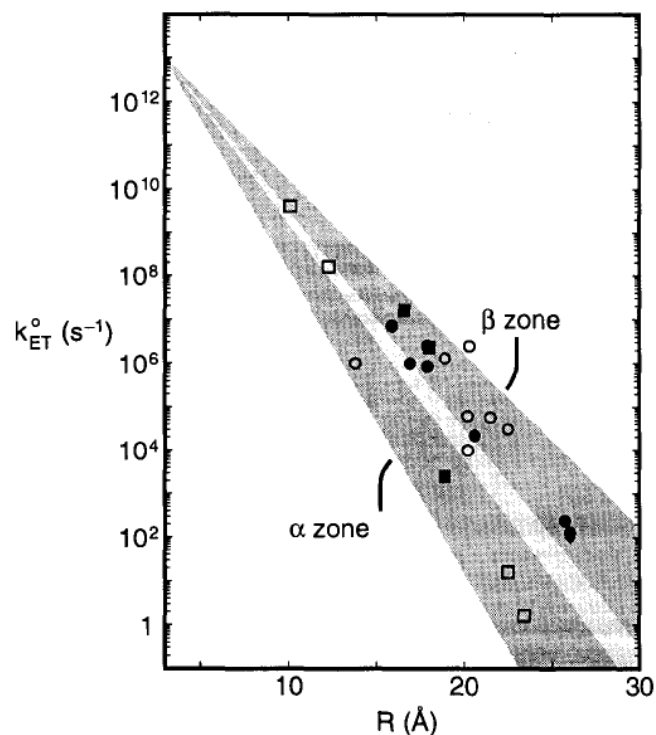


Various histidine substituted mutants for coordination with $\text{Ru}(\text{bpy})_2(\text{im})^{2+}$ on myoglobin, an α -helical protein

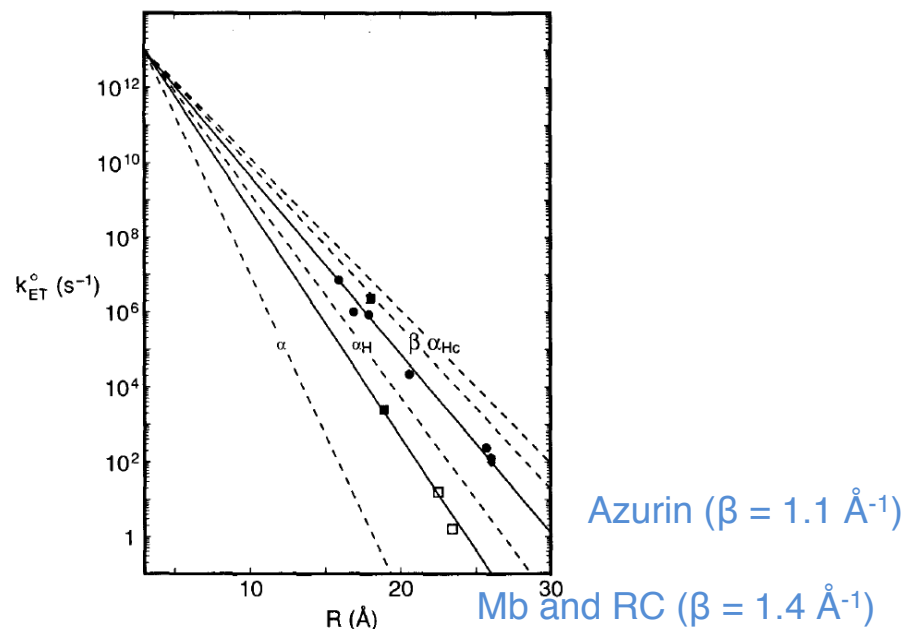


- ♦ Same analysis on two myoglobins (Mb) and the reaction center (RC) from the photosynthetic reaction center (PRC)
 - Measures electronic coupling across α -helix
- ♦ Obtained $\beta = 1.4 \text{ Å}^{-1}$,

Distance Dependence on an α -Helix



electron transfer rates through a variety of proteins

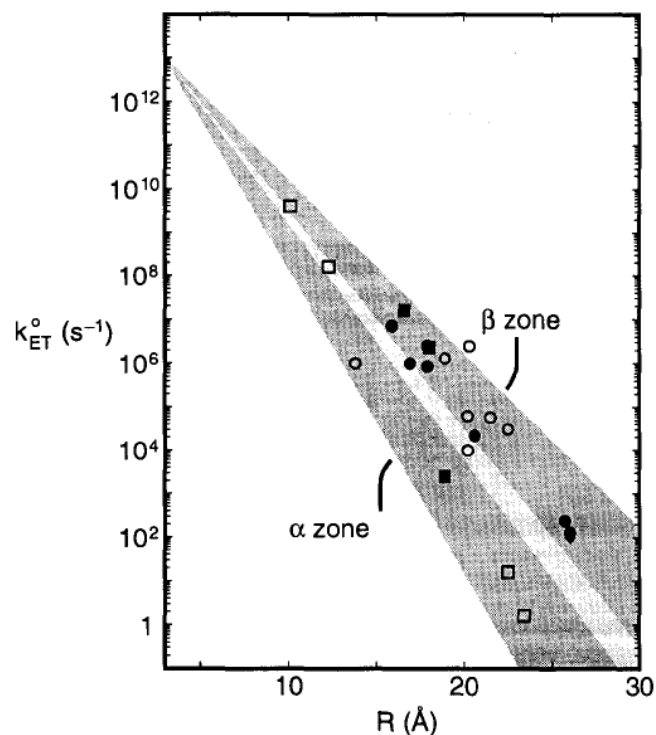


Azurin ($\beta = 1.1 \text{ Å}^{-1}$)

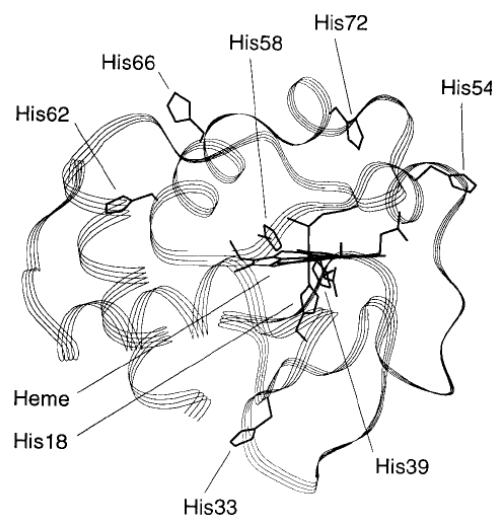
Mb and RC ($\beta = 1.4 \text{ Å}^{-1}$)

- ♦ The range around each slope define a secondary structure “zone”
- ♦ Plotting electron transfer on several proteins in this way, zones predict secondary structure well

Distance Dependence on an α -Helix



electron transfer rates through a variety of proteins



Various site-specific histidine mutants of cytochrome c, a protein with both α -helices and β -sheets

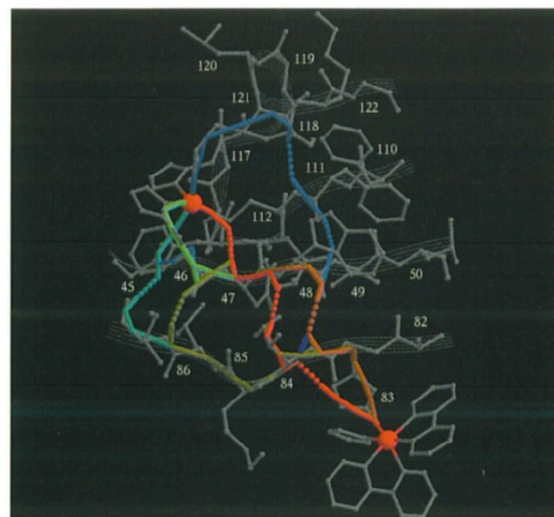
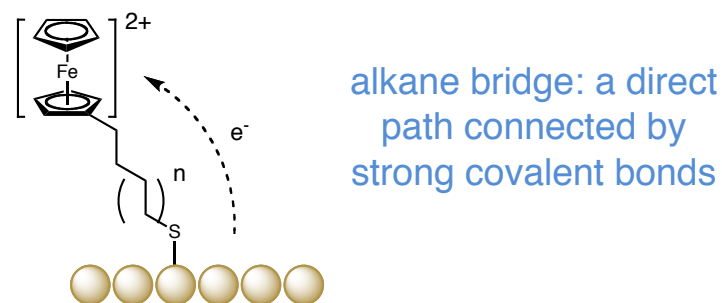
- ♦ The range around each slope define a secondary structure “zone”
- ♦ Plotting electron transfer on several proteins in this way, zones predict secondary structure well

How does secondary structure affect electronic coupling?

Gray, H.B.; Winkler, J.R. *Annu. Rev. Biochem.* **1996**, 65, 537-561.

Theoretical Analysis of Electronic Coupling

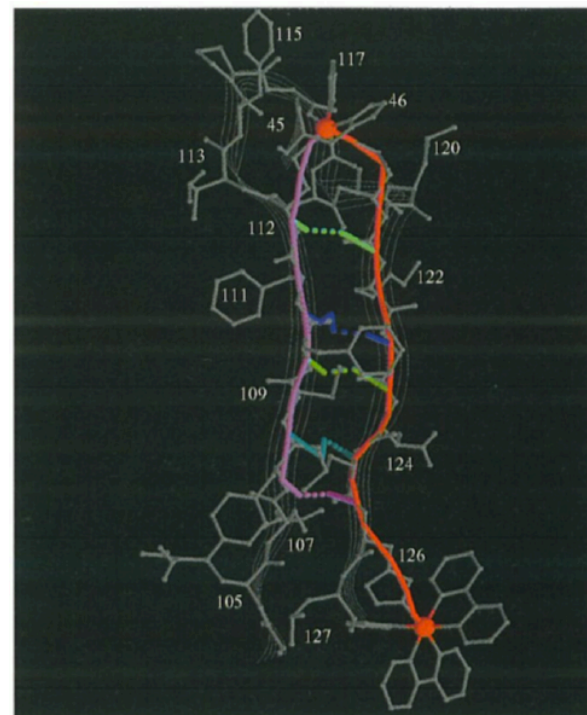
- ♦ Decay constants (β) determined by:
 - Barrier height (E of path)
 - Directness of path (effective distance)
 - Number of paths in 3-dimensions
- ♦ Computational approach:
 - Divide tunneling path into conduction zones connected by bonds, H-bonds, and through space jumps
 - Parameterize coupling decay for each link
 - Search algorithm identifies most likely path and coupling decays for each link



Theoretical Analysis of Electronic Coupling

Results:

- ♦ Conduction best through strong, covalent bonds
 - With hydrogen bonds, stronger bond means better conduction
 - Through space jumps have the highest coupling decays
- ♦ Effective tunneling distance (σ_l) depends on shape of the path
 - Longer for less direct routes



Tunneling pathways along the azurin backbone

Basis for Difference in Decay Constants

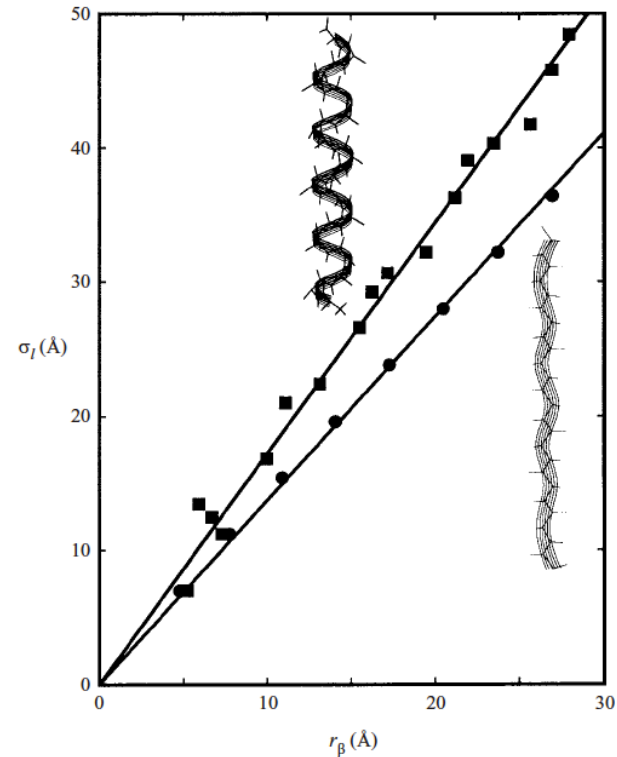
Comparison:

♦ α -helices:

- Weaker hydrogen bonds ($\nu_{\text{CO}} = 1680\text{-}1700\text{ cm}^{-1}$)
- Less direct pathway along backbone means greater effective tunneling distance (σ_l)
- Larger β , more “insulating”

♦ β -sheets:

- Stronger hydrogen bonds ($\nu_{\text{CO}} = 1630\text{ cm}^{-1}$)
- More direct pathway along backbone
- Smaller β , more “conducting”



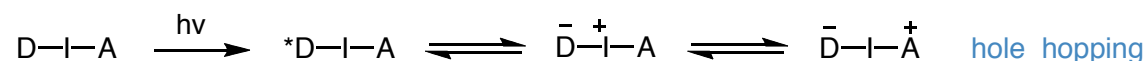
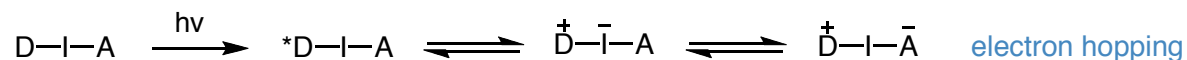
Calculated path length along
 α -helix and β -sheet

Conducting channels built into secondary structure provide directional control.

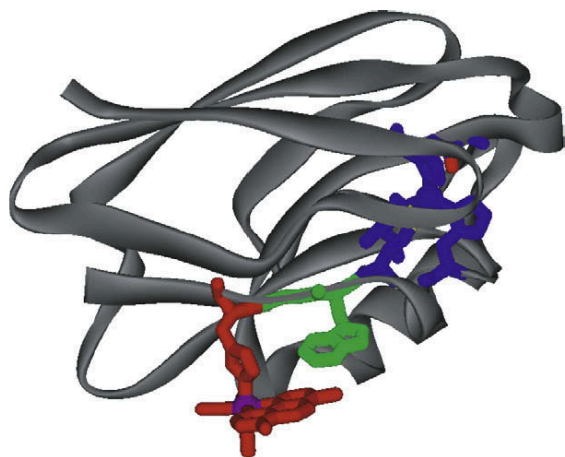
Regan, J.J.; DiBilio, A.J.; Langen, R.; Skov, L.K.; Winkler, J.R.; Gray, H.B.; Onuchic, J.N.; *Chem & Biol.* **1995**, 2, 489-496.

Hopping: a Mechanistic Alternative

Reaction scheme:



- ♦ Kinetics shows hopping is much more sensitive to temperature than single-step tunneling
- ♦ However, single-step tunneling over 20 Å is prohibitively slow in proteins, yet ET sometimes required over greater distances

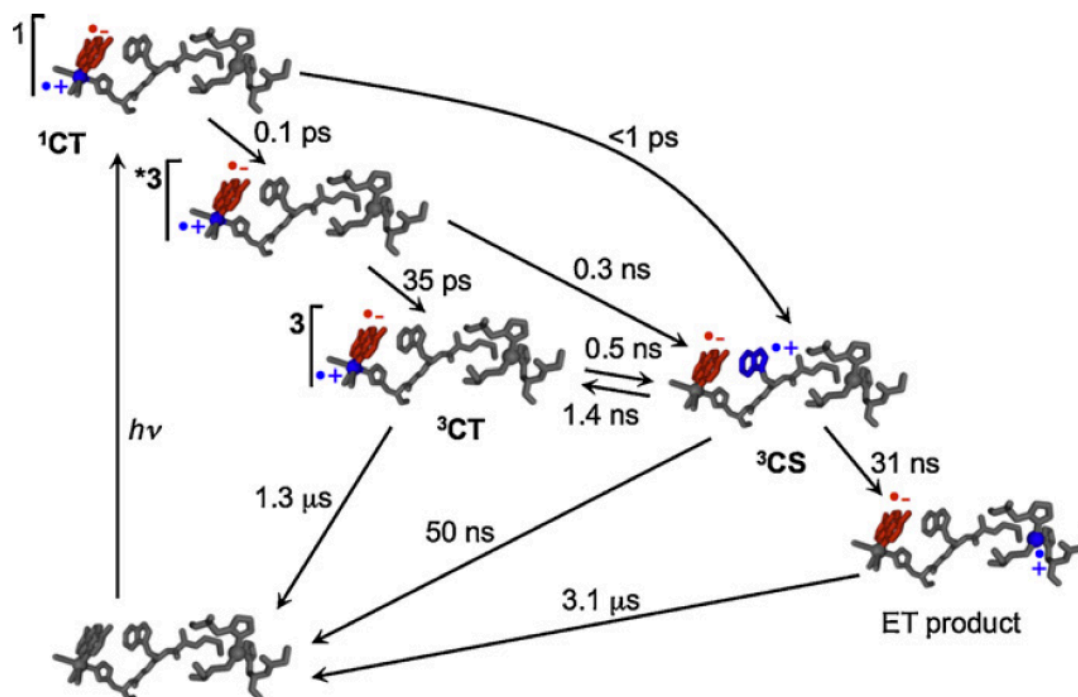


$\text{Re}^{\text{I}}(\text{CO})_3(\text{dmp})(\text{His124})(\text{Trp122})\text{AzurinCu}^{\text{II}}$

Objective:

- ♦ Observe hole hopping through an aromatic side chain in a suitably substituted azurin
- ♦ Identify structural features that control hopping in proteins

Hopping Through a Functionalized Azurin

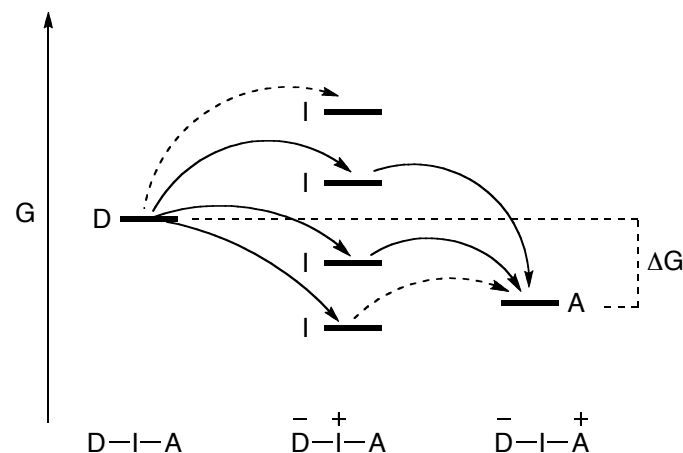
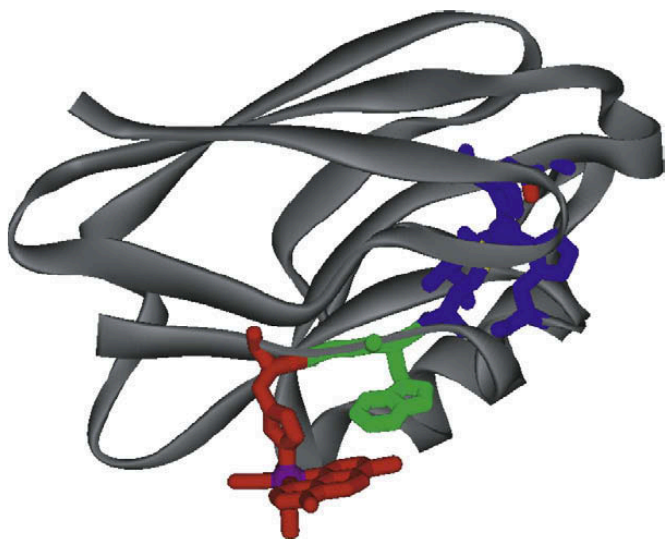


Hopping in $\text{Re}^I(\text{CO})_3(\text{dmp})(\text{His124})(\text{Trp122})\text{AzurinCu}^{II}$:

- ♦ Hopping route much faster than that predicted for single step ET (19 Å Re^I to Cu^{II})
- ♦ No hopping observed for Phe124, Tyr124, and Lys124 analogs
- ♦ Does not work for deprotonated indole (too exothermic for second ET)

Warren, J.J.; Ener, M.E.; Vlcek, A.; Winkler, J.R.; Gray, H.B. *Coord. Chem. Rev.* **2012**, 256, 2478-2487.

Hopping Through a Functionalized Azurin



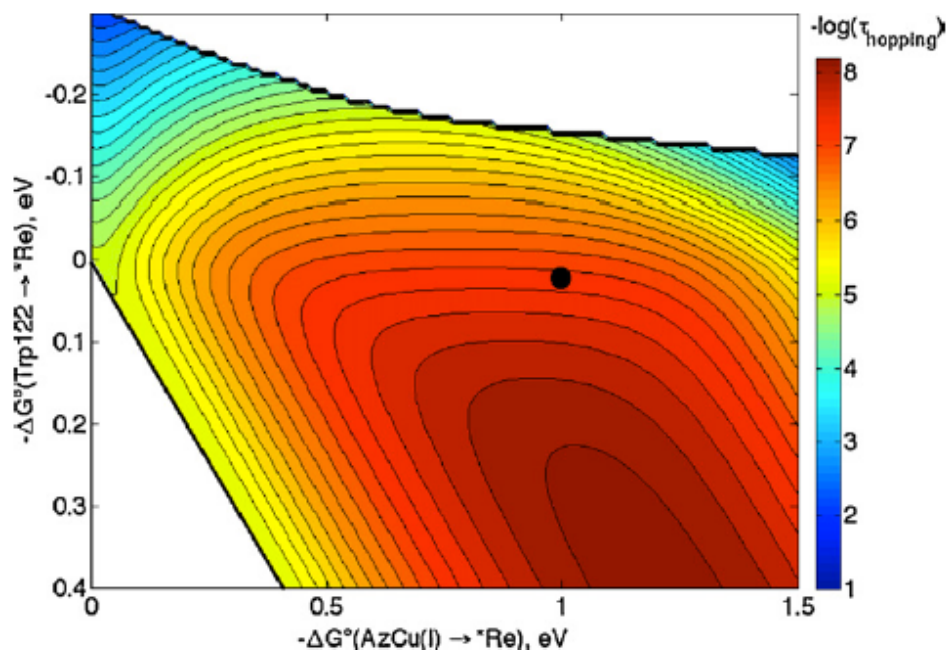
Alternative energy scenarios for hole hopping

- ♦ Oxidation-coupled deprotonation of indole would also make indole oxidation too exothermic
- ♦ No residues capable of directly deprotonating the indole, so it works at physiological pH

Hopping efficiency is very sensitive to the ΔG° of initial ET

Warren, J.J.; Ener, M.E.; Vlcek, A.; Winkler, J.R.; Gray, H.B. *Coord. Chem. Rev.* **2012**, 256, 2478-2487.

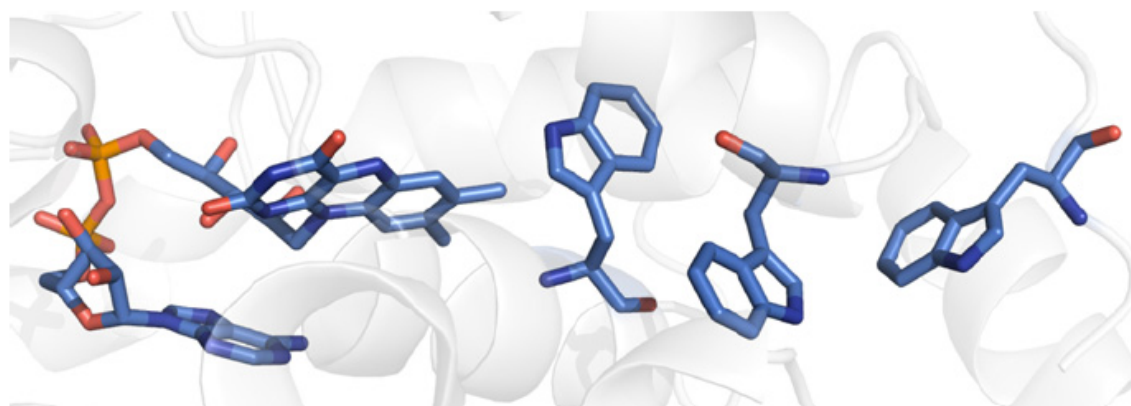
Hopping Maps For Substituted Azurins



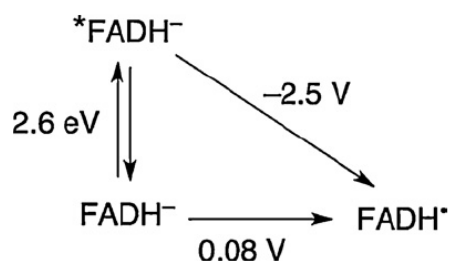
♦ Relationship between hopping rate and ΔG° for two steps can be modeled and represented with hopping maps

- Can determine for what ΔG° would hopping be faster than direct tunneling

Hopping in DNA Photolyase



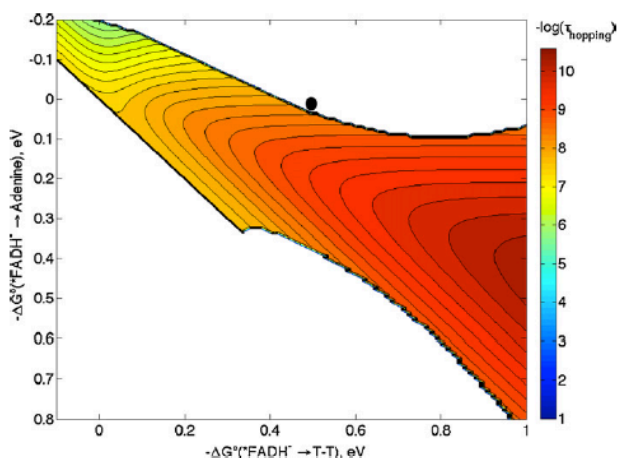
A hopping pathway for DNA photolyase?



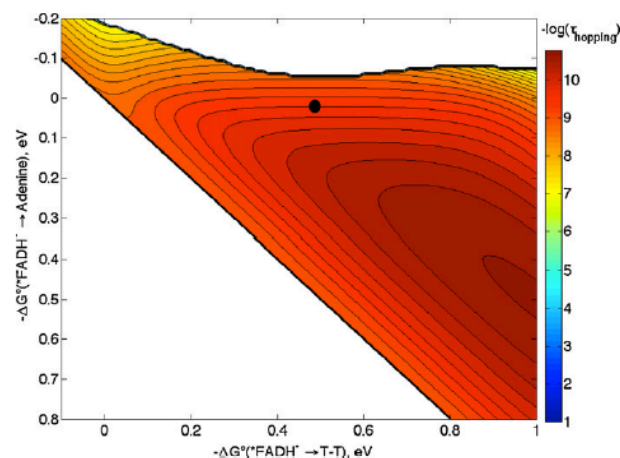
FADH⁻, a highly
reducing natural
photoredox catalyst

- ♦ DNA photolyase is involved in bacterial repair of UV-damaged DNA
- ♦ Site directed mutants show that all three tryptophans are required for substrate reduction
 - Also, no nearby base to deprotonate oxidized intermediates
- ♦ Initial computations suggest hopping mechanism too slow

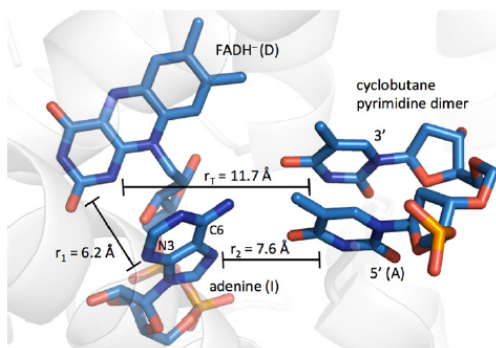
Hopping in DNA Photolyase



Hopping map with $\lambda = 0.8$ eV



Hopping map with $\lambda = 0.5$ eV

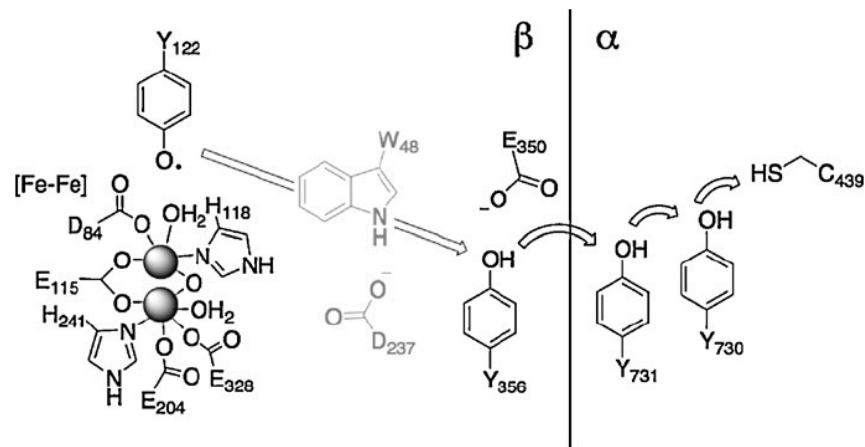


Proper reorganization energy
needed for hopping to work

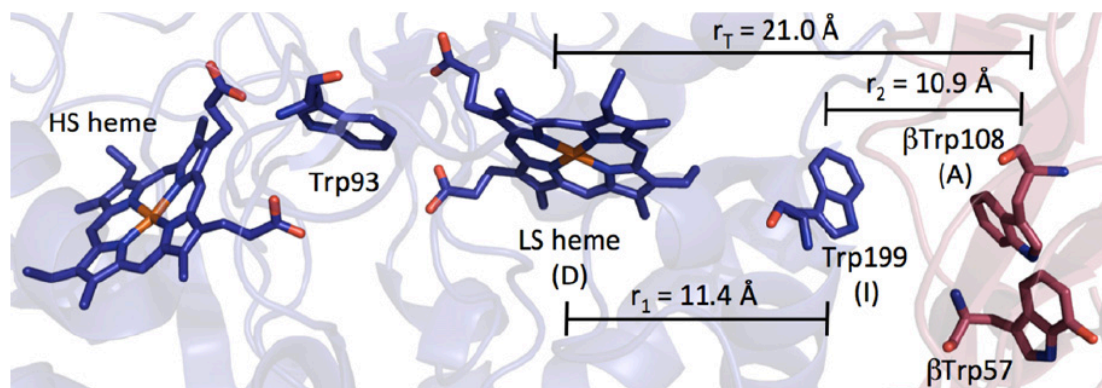
Hopping requires structural in addition to energetic fine tuning

Warren, J.J.; Ener, M.E.; Vlcek, A.; Winkler, J.R.; Gray, H.B. *Coord. Chem. Rev.* **2012**, 256, 2478-2487.

Hopping in Other Natural Systems

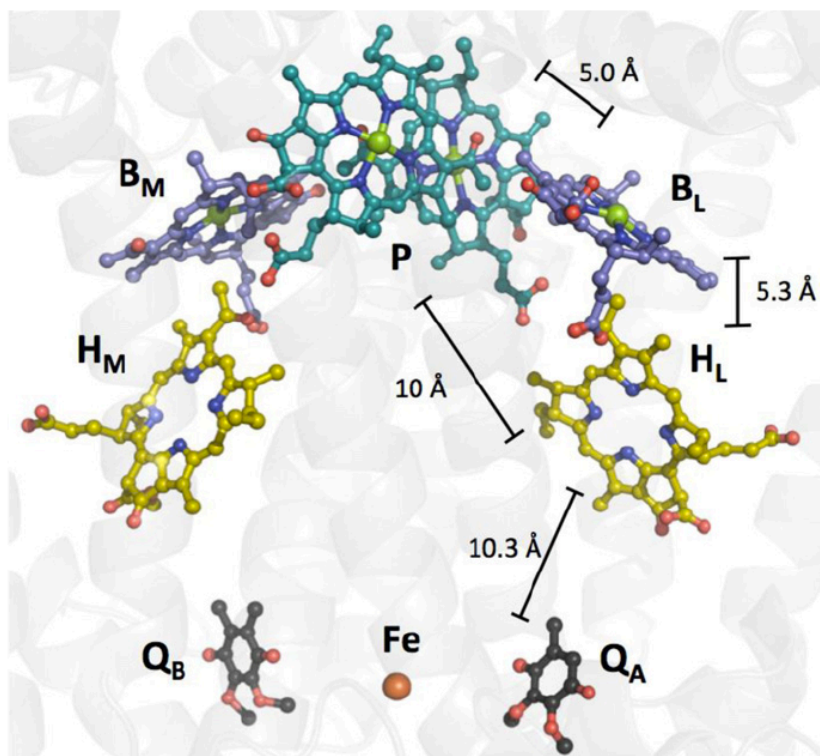


Proposed ET pathway in *E. coli* ribonucleotide reductase

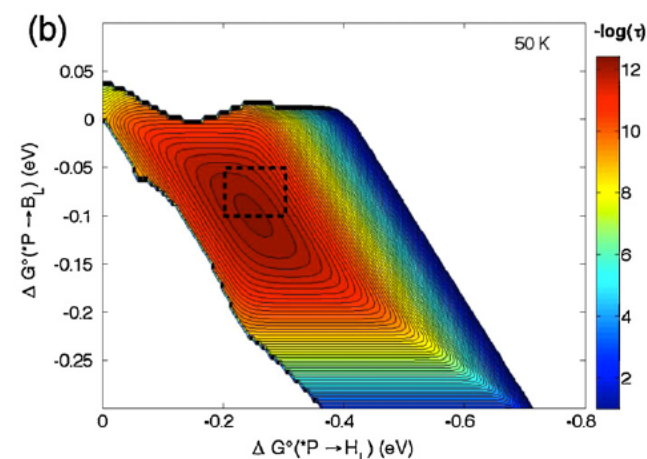


Tryptophans positioned for hopping in MauG

Hopping in the Photosynthetic Reaction Center



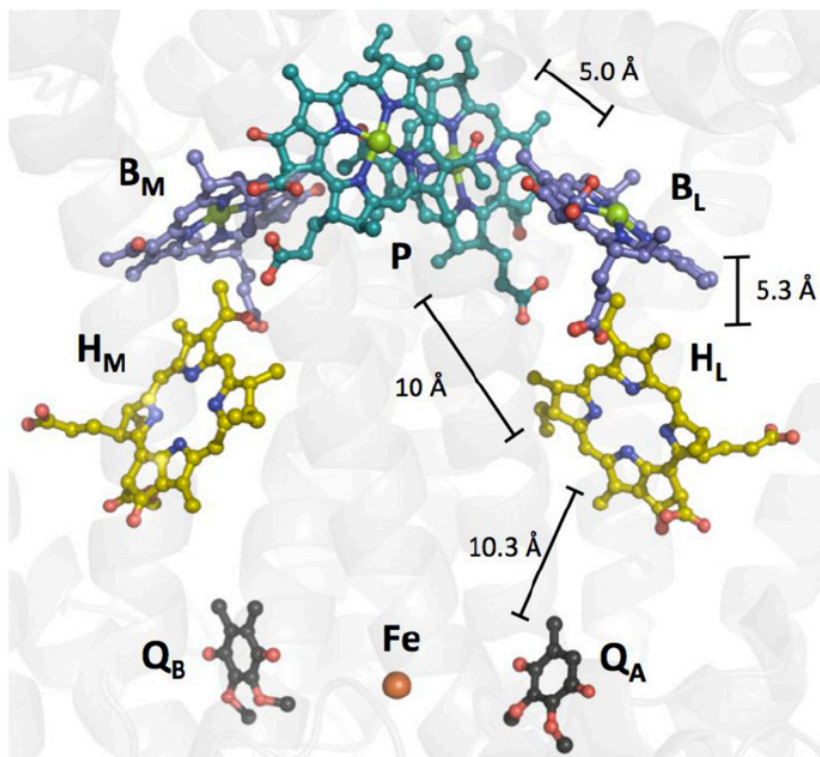
Bacterial photosynthetic reaction center. Special pair (P), bacteriochlorophyll (B), bacteriopheophytin (H), and quinone (Q)



Map for hopping through bacteriochlorophyll

- ♦ Hopping is an essential feature of ET transport in photosynthesis
 - Hopping maps suggest that ΔG° 's are highly optimized for hopping efficiency

Hopping in the Photosynthetic Reaction Center



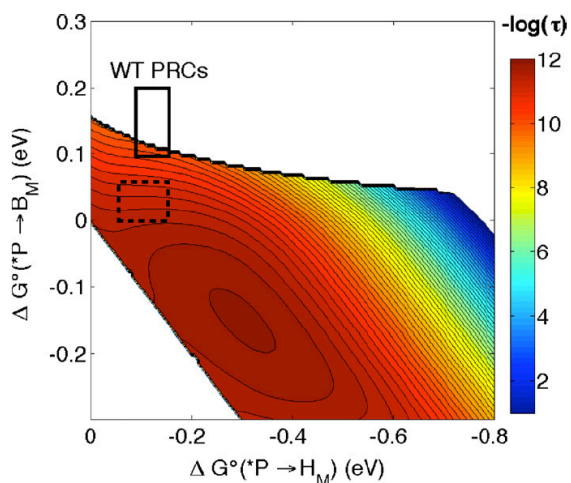
- ♦ Two branches, L and M, from the special pair
 - Same cofactors
 - Small difference in positioning and nearby amino acids
 - L branch is productive, but M completely inactive

What controls electron flow at this critical bifurcation in photosynthetic electron transfer?

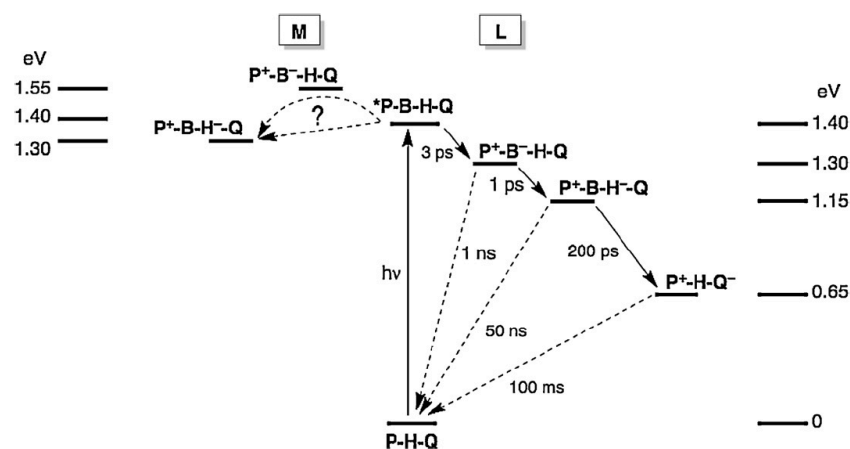
Bacterial photosynthetic reaction center. Special pair (P), bacteriochlorophyll (B), bacteriopheophytin (H), and quione (Q)

Hopping in the Photosynthetic Reaction Center

- ♦ Different amino acid environment results in slight changes in cofactor reduction potentials
 - Hopping maps suggest that ΔG° 's are poorly paired for hopping in the M branch
 - Direct electron transfer from the special pair (P_M) to bacteriopheophytin (H_M) too slow to make up for loss of hopping electron transfer



Map for hopping through bacteriochlorophyll in the M branch



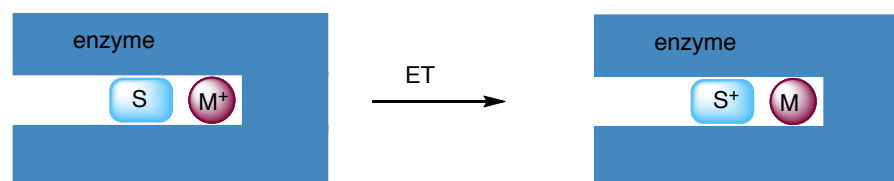
Measured energy levels in the M and L branch

Hopping with carefully optimized ΔG° 's controls electron flow in the PRC

Molecular Wires

Getting into the active site

- ♦ Electron transfer often occurs between enzyme-bound substrate and buried metal cofactor
- ♦ Electronic manipulation can be difficult from “outside” the protein because of long tunneling distances

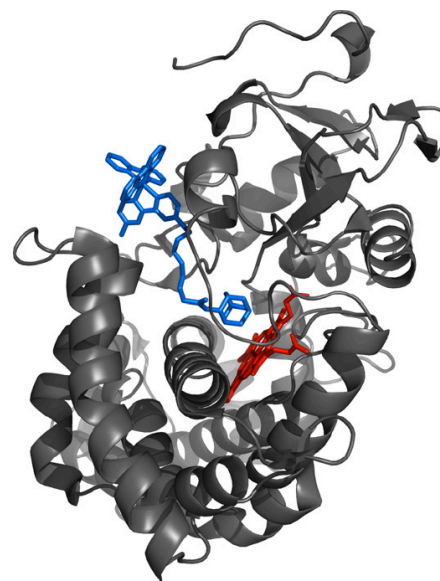
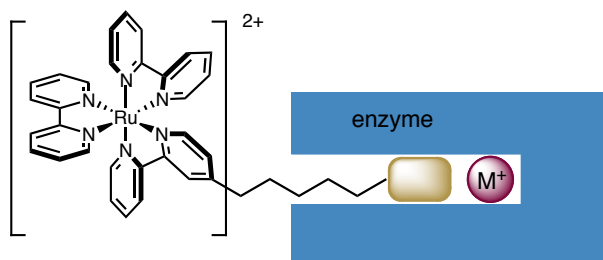


Electron transfer in a buried active site

Molecular Wires

Design Plan:

- ♦ Connect ligands with an affinity for active site to redox manipulable functional group outside the protein via an efficient tunneling wire

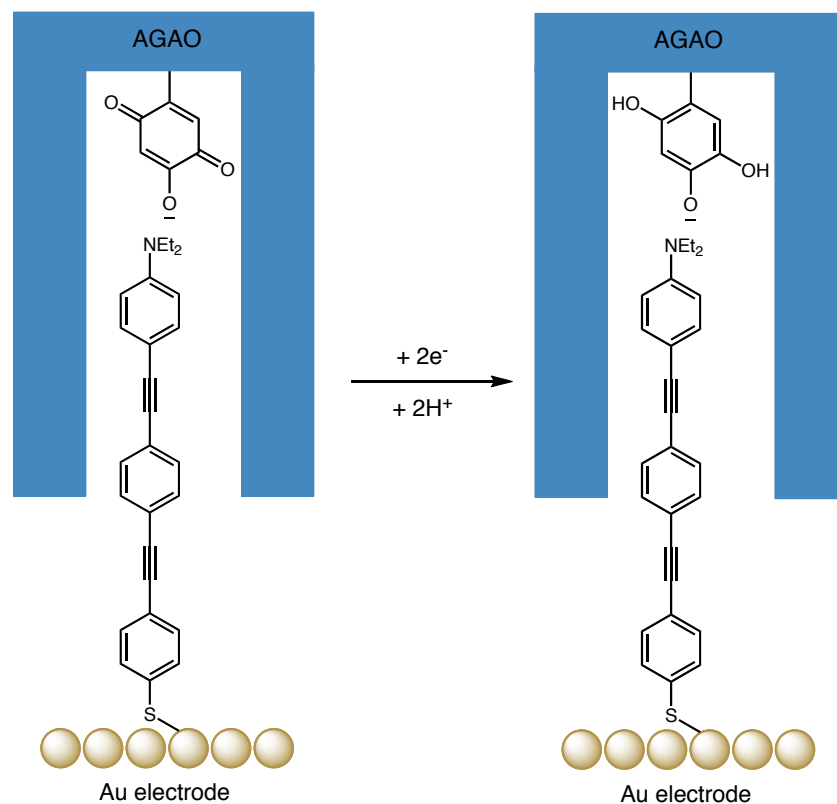


$\text{Ru}(\text{bpy})_3^{2+}$ connected to heme active site via molecular wire

Molecular Wires for Voltammetry

Measuring redox potentials

- ♦ *A. globiformis* amine oxidase (AGAO) oxidizes amines to aldehydes via an active site 2,4,6-trihydroxyphenylalanine quinone (TPQ)
- ♦ Measuring TPQ redox potentials not possible with standard electrode
- ♦ Molecular wire bridges 20Å hydrophobic channel to allow tunneling from electrode to TPQ
- ♦ $\beta = 0.4\text{-}0.6 \text{ \AA}^{-1}$ through phenylene-alkyne bridges

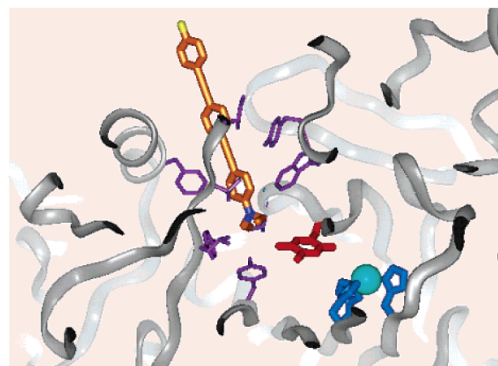


Molecular wires conduct electrons for cathodic reduction

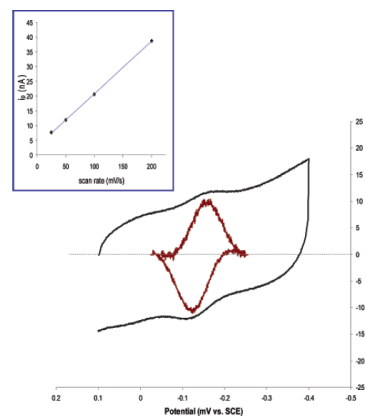
Molecular Wires for Voltammetry

Measuring redox potentials

- ♦ *A. globiformis* amine oxidase (AGAO) oxidizes amines to aldehydes via an active site 2,4,6-trihydroxyphenylalanine quinone (TPQ)
- ♦ Measuring TPQ redox potentials not possible with standard electrode
- ♦ Molecular wire bridges 20Å hydrophobic channel to allow tunneling from electrode to TPQ
 - ♦ $\beta = 0.4\text{-}0.6 \text{ \AA}^{-1}$ through phenylene-alkyne bridges



AGAO-molecular wire complex

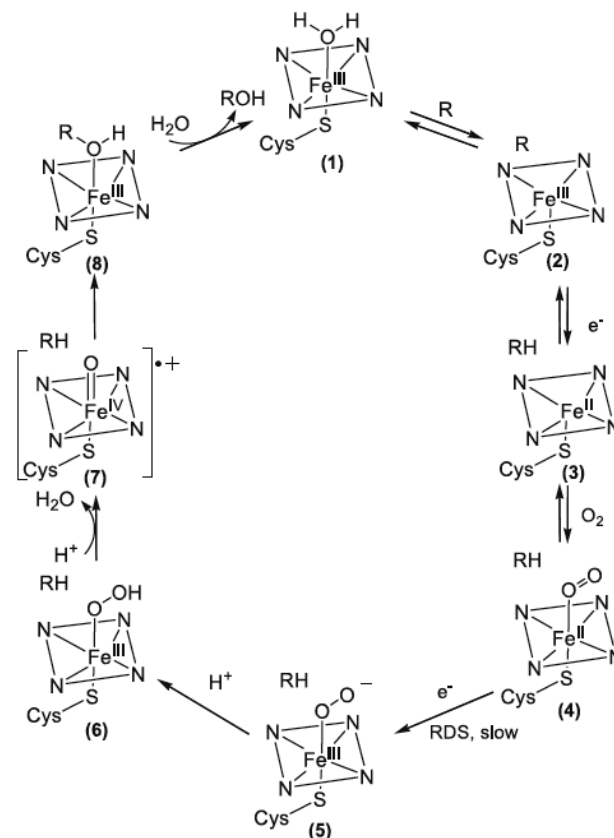


Successful CV run with molecular wire

Reduction of a Heme Cofactor

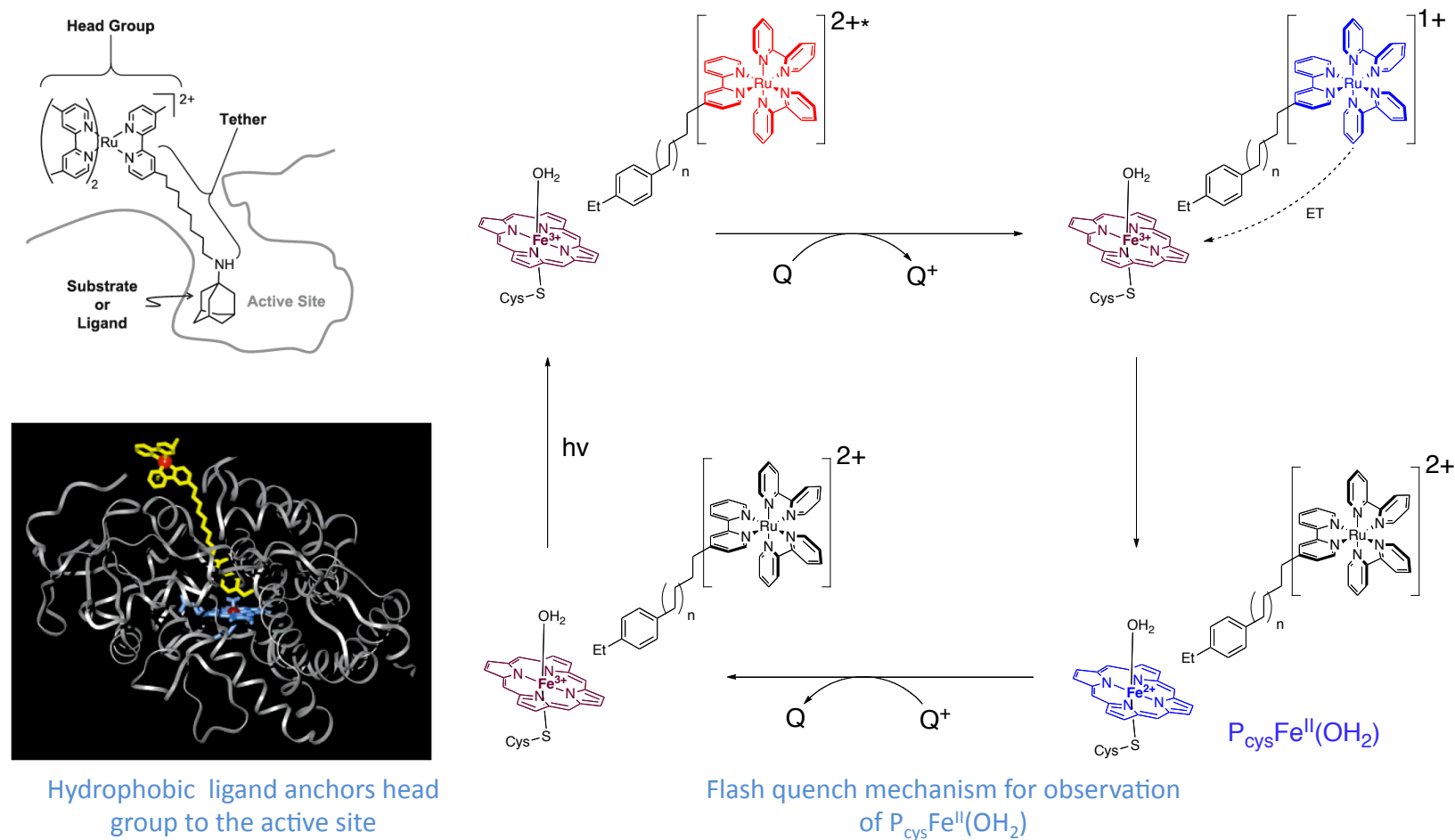
Heme oxidations in p450cam

- ◆ Efficient for hydroxylation of hydrophobic substrates, especially camphor (hence “cam”)
- ◆ Mechanism of heme oxidations well-studied and key intermediates like oxoferryl (7) characterized
- ◆ Transient intermediates, such as reduced $P_{\text{cys}}\text{Fe}^{\text{II}}(\text{OH}_2)$ (3) cannot be isolated or observed under reaction conditions



Currently accepted mechanism for
p450 hydroxylations

Flash-Quench Reduction of a Heme Cofactor



Photoreduction through a tunneling wire allows observation of $P_{\text{cys}}\text{Fe}^{\text{II}}(\text{OH}_2)$

Hartings, M.R.; Kurnikov, I.V.; Dunn, A.R.; Winkler, J.R.; Gray, H.B.; Ratner, M.A. *Coord. Chem. Rev.* **2010**, 254, 248.

Summary

- ◆ Efficient electron transfer in biological systems involves
 - Fixed coordination and solvent exclusion to minimize reorganization energies (λ)
 - Conduction channels built into secondary structure
 - Hopping through intermediates optimally positioned spatially and energetically
- ◆ A model was developed for predicting the energetic requirements for hopping in a redox machine
- ◆ These principles were used to design molecular wires for redox manipulation of buried active site cofactors

In addressing high impact problems in energy conversion and fuel technology, the principles of efficient electron transfer will be essential to chemical solutions to tomorrow's technology needs.